

On the Effectiveness of Quasi-Helmholtz Projectors in Preconditioning Problems with Junctions

Johann Bourhis⁽¹⁾, Andrien Merlini⁽²⁾, and Francesco P. Andriulli⁽¹⁾

⁽¹⁾ Politecnico di Torino, Turin, Italy

⁽²⁾ IMT Atlantique, Brest, France

Abstract—The electric field integral equation (EFIE) is known to suffer from ill-conditioning and numerical instabilities at low frequencies (low-frequency breakdown). A common approach to solve this problem is to rely on the loop and star decomposition of the unknowns. Unfortunately, building the loops is challenging in many applications, especially in the presence of junctions. In this work, we investigate the effectiveness of quasi-Helmholtz projector approaches in problems containing junctions for curing the low-frequency breakdown without detecting the global loops. Our study suggests that the performance of the algorithms required to obtain the projectors in the presence of junctions are maintained while keeping constant the number of sheets per junction. Finally, with a sequence of numerical tests, this work shows the practical impact of the technique and its applicability to real case scenarios.

I. INTRODUCTION

The electric field integral equation (EFIE) provides the solution of electromagnetic scattering and radiation problems for perfectly electrically conducting (PEC) objects. At low-frequency, the unbalanced coefficients scaling of the EFIE lead to ill-conditioned linear systems and to numerical instabilities [1]. This is the so-called low-frequency breakdown and it is standardly solved using quasi-Helmholtz approaches such as loop and star decomposition [1] where the unknowns are separated into their solenoidal and non-solenoidal parts. These decompositions require to search for global loops, a challenge even when junctions are not present. This search however, is substantially more complicated when junctions are present, since the number of global cycles grows fast [2].

In this work we analyse and extend the use of quasi-Helmholtz projectors to low frequency EFIE problems containing junctions. We first show that the orthogonality between the solenoidal and non-solenoidal projectors is not compromised by the presence of junctions. Hence, the non-solenoidal projector obtained in the case of junctions gives rise by complementarity to the correct solenoidal space. A computation of the projectors using algebraic multigrid (AGMG) [3] is analyzed numerically. Our results show that the efficiency of this algorithm is not jeopardized when the number of junctions grows, provided that the number of insertions per junction remains constant. This is in agreement with the spectral properties of graph Laplacians [4]. Finally, we give numerical results to illustrate the effectiveness of the proposed approach and its applicability to relevant scenarios.

II. BACKGROUND AND NOTATIONS

We want to determine the electric field \mathbf{E}^{sct} scattered by a perfect electric conducting (PEC) boundary Γ on which

impinges a field \mathbf{E}^{inc} in a medium of characteristic impedance η . We assume the fields to be time-harmonic with wavenumber κ . The EFIE is derived from Maxwell's equations considering a surfacic electric current density \mathbf{J} induced over Γ from which \mathbf{E}^{sct} can be computed outside Γ . Following the boundary element method, we discretize the current $\mathbf{J}(\mathbf{r}) \approx \sum_{i=1}^N [\mathbf{j}]_i \boldsymbol{\varphi}_i(\mathbf{r})$, where $\boldsymbol{\varphi}_i$ are Rao-Wilton-Glisson (RWG) basis functions defined on a triangular mesh. After testing, we obtain a $N \times N$ linear system

$$\left(i\kappa \mathbf{Z}_s + \frac{1}{i\kappa} \mathbf{Z}_h \right) \mathbf{j} = \mathbf{e}, \quad (1)$$

where $[\mathbf{Z}_s]_{ij} = \langle \mathbf{n} \times \boldsymbol{\varphi}_i, \mathcal{T}_{A,\kappa} \boldsymbol{\varphi}_j \rangle$, $[\mathbf{Z}_h]_{ij} = \langle \mathbf{n} \times \boldsymbol{\varphi}_i, \mathcal{T}_{\phi,\kappa} \boldsymbol{\varphi}_j \rangle$ and $[\mathbf{e}]_i = -\frac{1}{\eta} \langle \mathbf{n} \times \boldsymbol{\varphi}_i, \mathbf{n} \times \mathbf{E}^{\text{inc}} \rangle$, with $\langle f, g \rangle = \int_{\Gamma} f(\mathbf{r})g(\mathbf{r}) dS(\mathbf{r})$. The operators $\mathcal{T}_{A,\kappa}$ and $\mathcal{T}_{\phi,\kappa}$ are the rotated vector and scalar potentials on the surface [1] and \mathbf{n} is the oriented unit normal over Γ . On edges that form a junction between n triangles, we define $n - 1$ independent RWGs on $n - 1$ couples of triangles as is often done [2].

The loop and star basis functions can be mapped from the RWGs by constructing transformation matrices [1]. Even if the matrix mapping the local loops can always be defined by association to the vertices of the mesh, its construction requires particular attention with junctions and open boundaries. By analogy to the RWGs, we have to eliminate the external nodes and to define additional loops for each plan formed around a junction. Furthermore, it is known that the seeking of the global loops often represents a substantial computational cost. Unfortunately, the presence of multiple junctions can increase the number of “non-harmonic” global cycles (see the structures in Fig. 1 and Fig. 2) that being associated to an open boundary instead of a point still need to be detected.




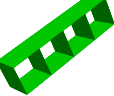
III. QUASI-HELMHOLTZ PROJECTORS WITH JUNCTIONS

The transformation matrix which maps the stars into the RWG space can be defined in the case of junctions like in the standard case as

$$[\boldsymbol{\Sigma}]_{ij} = \begin{cases} 1 & \text{if } \nabla \cdot \boldsymbol{\varphi}_i(\mathbf{r}) > 0 \text{ on the triangle } j, \\ -1 & \text{if } \nabla \cdot \boldsymbol{\varphi}_i(\mathbf{r}) < 0 \text{ on the triangle } j, \\ 0 & \text{otherwise.} \end{cases} \quad (2)$$

With these functions, the orthogonality between the solenoidal and non-solenoidal spaces is preserved by construction and their completeness can equally be shown. This can be seen considering the graph associated to $\boldsymbol{\Sigma}$. This graph represents the connexions between the triangles (vertices) formed by the

TABLE I
NUMBER OF ITERATIONS ACHIEVED BY AGMG FOR INCREASING
DISCRETIZATION WITH A RESIDUAL ERROR BELOW $1 \cdot 10^{-8}$.

Structure	Unknowns	Iter.	Structure	Unknowns	Iter.
	$7.2 \cdot 10^3$	21		$2.9 \cdot 10^3$	18
	$6.9 \cdot 10^4$	22		$2.8 \cdot 10^5$	24
	$7.0 \cdot 10^5$	22		$2.7 \cdot 10^6$	22
	$6.9 \cdot 10^6$	23		$2.8 \cdot 10^7$	23
	$1.2 \cdot 10^3$	18		$3.2 \cdot 10^3$	19
	$1.2 \cdot 10^5$	22		$3.0 \cdot 10^5$	22
	$1.2 \cdot 10^6$	23		$3.0 \cdot 10^6$	23
	$1.2 \cdot 10^7$	23		$3.0 \cdot 10^7$	25

RWGs (edges). The vertices (mesh triangles) and the faces (internal mesh nodes and cycles along open boundaries) are respectively associated to the stars and to the loops (this is a dual graph). We denote by N , S , and L the number of edges, vertices and faces of this graph. To work with the same general formula for open structures, the exterior domain is counted as one face and does not correspond to any loop. For closed structures, we also have to account for the H handles that correspond to the discrete harmonic subspace. The Euler-Poincaré formula establishes $N = S + L + 2(H - 1)$. Moreover, the number of independent stars is always $S - 1$ which impacts the rank of Σ and the dimension of its orthogonal space $L - 1 + 2H$ which is the right number of independent loops.

The orthogonality between the quasi-Helmholtz spaces eliminates the need for seeking loops and cycles. In fact, the quasi-Helmholtz projectors of the non-solenoidal and solenoidal spaces are respectively calculated as $P_\Sigma = \Sigma(\Sigma^T \Sigma)^+ \Sigma^T$ and $P_{\Lambda H} = I - P_\Sigma$, where “+” denotes the Moore-Penrose pseudoinverse. Subsequently, we cure the low-frequency breakdown by defining a preconditioner $P = \frac{1}{\sqrt{\kappa}} P_{\Lambda H} + i\sqrt{\kappa} P_\Sigma$ which yields to a system with a bounded condition number at low-frequencies

$$P \left(i\kappa Z_s + \frac{1}{i\kappa} Z_h \right) P y = P e, \quad \text{with } j = P y. \quad (3)$$

IV. GRAPH LAPLACIANS WITH JUNCTIONS

Preconditioning the EFIE with the quasi-Helmholtz projectors requires the iterative inversion of the graph Laplacian $\Sigma^T \Sigma$. This can be efficiently done via AGMG. In this work, we have numerically verified that AGMG remains accurate with a complexity in $\mathcal{O}(N \log(N))$ operations even for really dense discretized problems containing several junctions. This is illustrated in Table I which shows that the number of iterations of the AGMG process increases logarithmically with the number of unknowns when the maximal number of sheets per junction remains constant. It should be noted, however, that the largest eigenvalue of $\Sigma^T \Sigma$ increases with the maximal degree of the graph, that is the maximal number of interconnected triangles [4]. As a consequence, AGMG may fail for structures containing an increasing number of sheets per junction, while performance does not deteriorate when this number remains constant.

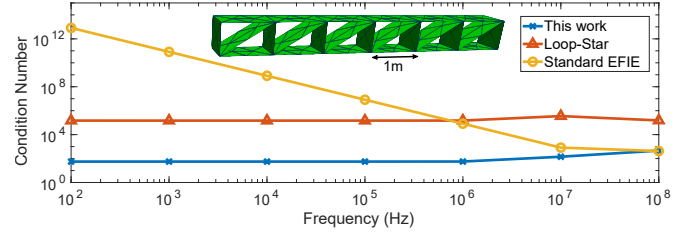


Fig. 1. Comparison of the condition number of the EFIE matrix with or without preconditioning from medium to low frequency.

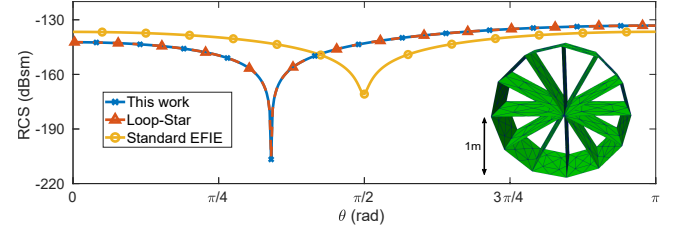


Fig. 2. Radar Cross Section (RCS) obtained with and without preconditioning with a frequency of $1 \cdot 10^4$ Hz. The structure is irradiated by a plane wave.

V. NUMERICAL RESULTS

In our numerical results, we have used two models of structures containing different types and numbers of junctions. Results obtained by solving the EFIE with and without preconditioning from medium to low frequencies are compared along with the loop-star decomposed EFIE [1]. The condition number of the linear systems as a function of the frequency is reported in Fig. 1. The preconditioned matrices clearly remain well-conditioned when the frequency decreases, while the condition number drastically increases for the standard formulation. In addition, the quasi-Helmholtz projectors show a better conditioning than the loop-star decomposition thanks to their flat spectrum. Fig. 2 shows that the proposed formulation and the loop-star formulation yield comparable results at low-frequency, unlike the standard formulation.

ACKNOWLEDGMENT

This work was supported in part by the European Research Council (ERC) through the European Union’s Horizon 2020 Research and Innovation Programme under Grant 724846 (Project 321) and in part by the H2020-MSCA-ITN-EID project COMPETE GA No 955476.

REFERENCES

- [1] S. B. Adrian, A. Dely, D. Consoli, A. Merlini, and F. P. Andriulli, “Electromagnetic integral equations: Insights in conditioning and preconditioning,” *IEEE Open Journal of Antennas and Propagation*, 2021.
- [2] P. Ylä-Oijala, M. Taskinen, and J. Sarvas, “Surface integral equation method for general composite metallic and dielectric structures with junctions,” *Progress In Electromagnetics Research*, vol. 52, pp. 81–108, 2005.
- [3] A. Napov and Y. Notay, “An efficient multigrid method for graph Laplacian systems II: Robust aggregation,” *SIAM Journal on Scientific Computing*, vol. 39, no. 5, pp. 379–403, 2017.
- [4] X.-D. Zhang, “The Laplacian eigenvalues of graphs: A survey,” *Linear Algebra Research Advances*, 2011.